Evaluation of a Noninvasive Command Scheme for Upper-Limb Prostheses in a Virtual Reality Reach and Grasp Task

Rahul R. Kaliki*, Rahman Davoodi, and Gerald E. Loeb, *Senior Member, IEEE*

***Abstract*—C5/C6 tetraplegic patients and transhumeral amputees may be able to use voluntary shoulder motion as command signals for a functional electrical stimulation system or transhumeral prosthesis. Stereotyped relationships, termed "postural synergies," among the shoulder, forearm, and wrist joints emerge during goal-oriented reaching and transport movements as performed by able-bodied subjects. Thus, the posture of the shoulder can potentially be used to infer the desired posture of the elbow and forearm joints during reaching and transporting movements. We investigated how well able-bodied subjects could learn to use a noninvasive command scheme based on inferences from these postural synergies to control a simulated transhumeral prosthesis in a virtual reality task. We compared the performance of subjects using the inferential command scheme (ICS) with subjects operating the simulated prosthesis in virtual reality according to complete motion tracking of their actual arm and hand movements. Initially, subjects performed poorly with the ICS but improved rapidly with modest amounts of practice, eventually achieving performance only slightly less than subjects using complete motion tracking. Thus, inferring the desired movement of distal joints from voluntary shoulder movements appears to be an intuitive and noninvasive approach for obtaining command signals for prostheses to restore reaching and grasping functions.**

***Index Terms*—Amputee, C5/C6, grasping, neural networks, quadriplegic, reaching, synergies, transhumeral, upper-limb prostheses, virtual reality (VR).**

I. Introduction

CURRENT upper-limb prosthetic options for quadriplegics and transhumeral amputees are quite limited. To restore meaningful functionality to these patients, a prosthesis must restore the control of at least five degrees of freedom (DOF): the specification of the hand position in extrapersonal space (3 DOF), the orientation of the hand about the longitudinal axis of the forearm, and the opening and grasping functions of the hand. Mechatronic prostheses can provide required movement, but they are difficult to control. This is because there are more motors to control than there are command signals to control them. Thus, the simple task of reaching and grasping that able-bodied humans take for granted becomes a complicated sequence of switching between output DOFs and making incremental adjustments until the task is complete. Many unilateral amputees abandon their prosthetic limbs, citing difficulties in control and functionality [1].

In fact, the various DOFs of the intact human arm and hand tend not to be used completely independently. Reaching movements tend to have a high degree of stereotypical behavior among joints and across the workspace. Several studies have shown that the movement of the hand generally follows a straight line with a bell-shaped velocity curve irrespective of speed during unimpeded reaching [2]–[7]. These properties emerge despite the number of redundant DOFs in the upper limb. Furthermore, when the initial position of the hand is controlled, highly reproducible relationships exist between the proximal and distal joint angles of the upper limb during reaching [5], [8], [9]. We and others have termed these relationships "postural synergies."

In previous work [10], [11], we laid a foundation for an intuitive and noninvasive inferential command scheme (ICS) for upper-limb prostheses that takes advantage of these postural synergies. It is based on inferring the desired posture of the distal joints of the arm from the residual voluntary movements of the shoulder, which are largely intact in transhumeral amputees and most C5/C6 quadriplegic patients. We showed that, using offline data from able-bodied subjects, artificial neural networks (ANNs) can predict most of the stereotyped postural synergies that emerge from the coordination of upper-limb joints during reaching to locations away from the body.

However, the restoration of reaching abilities alone is not functionally beneficial. As discussed earlier, a prosthesis must also restore the abilities to orient and open/close the hand. Furthermore, in our previous work, the ICS was only able to predict reaches away from the body. Thus, reaches directed near the mouth, as one would need to perform during eating or drinking, were not possible. To address these issues, we have modified our approach to leverage the unused translational DOF of the sternoclavicular joint and mapped them to the necessary upper-limb functions.

Offline analysis merely shows whether or not an exploitable relationship exists and can be extracted by ANNs. It does not, however, give any indication as to how well a human can overcome intrinsic errors of a pretrained algorithm and learn a novel control scheme to operate a prosthetic device during everyday tasks. Evidence from psychophysical experiments has shown

Manuscript received April 3, 2011; accepted June 7, 2011. Date of publication January 23, 2012; date of current version March 7, 2013. This work was supported by the National Science Foundation Engineering Research Center for Biomimetic MicroElectronic Systems under Grant EEC-0310723. *Asterisk indicates corresponding author*.

*R. R. Kaliki is with Infinite Biomedical Technologies, Baltimore, MD 21218 USA (email: rahul@i-biomed.com).

R. Davoodi and G. E. Loeb are with the Department of Biomedical Engineering, University of Southern California, Los Angeles, CA 90089 USA (e-mail: davoodi@usc.edu; gloeb@usc.edu).

Color versions of one or more of the figures in this paper are available online at http://ieeexplore.ieee.org.

Digital Object Identifier 10.1109/TBME.2012.2185494

that human subjects can learn to produce straight hand paths despite initial errors resulting from kinematic or dynamic perturbations [12]–[14]. Thus, we hypothesize that given both a reasonable and a consistent estimate of the desired outputs, subjects should learn to cope with errors by modifying their shoulder movements to complete the reach and grasp tasks successfully.

This study examines the ability of able-bodied subjects to use the ICS based on shoulder movements to perform a set of reach and grasp tasks in a virtual reality environment (VRE) [15]. Specifically, we have designed a virtual reality (VR) task to mimic the problem of reaching to and grasping a bottle and bringing it to the mouth. This task requires the subject to reach to bottle in 3-D space, orient the hand to match the orientation of the bottle, grasp the bottle, and, then, position the item near the mouth.

One significant issue presented by this approach is that patients who already have amputations or paralysis will be unable to generate reaching movements with which to train an ANN. Thus, we also need to evaluate whether subjects can learn to use ANNs trained on another subject's reaching data. Assuming that the neural networks give a reasonable estimate of synergies that are similar in all subjects, we hypothesized that there would not be a significant difference in performance when switching between networks trained with their own data and networks trained with another subject's data. In order to quantify performance with the ICS, various metrics were used to compare learning rates and performance in a group of able-bodied subjects using the ICS ("ICS group") versus a group of subjects using complete motion capture from their intact arm movements ("control group") to control an animated arm in the same VR task. Both groups of subjects had to learn to use the VRE, so differences between them should reflect performance limitations expected for an actual prosthetic system.

II. Methods

Eight able-bodied subjects participated in the experiments. Prior to training the ANNs, joint angle data were recorded as each subject performed reaches to a handle placed in random positions and orientations within extrapersonal space. ANNs were trained and evaluated offline. Each subject, then, performed a VR reach and grasp task using either the ICS control or direct mapping from the motion control system.

A. Motion Tracking Procedure

A Flock of Birds (Ascension Technologies Corporation, Burlington, VA) motion capture system was used to record the joint angles of each subject's right arm at 100 samples/s. Subjects had sensors placed on the acromion, on the upper arm above the elbow, and proximal to the wrist on the forearm. Prior to experimentation, calibration was done to compensate for any misalignments between the sensors and the segments they were tracking. Each sensor measures position and orientation (as rotation matrices) with respect to the base transmitter. Clinically meaningful Euler angles were derived from the rotation matrices, including shoulder abduction/adduction $\mathrm{S_{ABAD}}$, shoulder flexion/extension $\mathrm{S_{FE}}$, and shoulder internal external rotation $\mathrm{S_{IER}}$. The other recorded angles were sternoclavicular depression/elevation $\mathrm{SC_{DE}}$, sternoclavicular protraction/retraction $\mathrm{SC_{PR}}$, elbow flexion/extension $\mathrm{E_{FE}}$, and radioulnar pronation/supination $\mathrm{F_{PS}}$. A more detailed description of the calibration methodology and angle extraction algorithm can be found in [16].

B. Training Data Acquisition and Processing

Training the ICS requires a systematic dataset consisting of normal reach and grasp movements made to targets at various positions and orientations throughout extrapersonal space. A large robotic gantry (Parker Hannifin, Corporation, Mayfield Heights, OH) was used to automate the presentation of targets within a 2 m $\times$ 1 m $\times$ 1 m 3-D workspace. At the working end of the gantry arm, a cylindrical handle was actuated by a stepper motor and rotated to one of four orientations (0°, 45°, 90°, or 135° in the frontal plane). Prior to experimentation, target locations were scaled to the subject's physical measurements. Targets were located within a range of 60–100% of the measured arm lengths away from the shoulder center of rotation. Target locations were limited to this range because reaches to targets located proximally to this range required very little contribution from the shoulder, resulting in poor predictability of the distal joint angles. A more detailed description of the methodology used to determine the distribution of target locations can be found in [10].

At the onset of the data acquisition trials, subjects were seated in a high back chair and secured with elastic bands around the torso to limit movement of the trunk during experimentation. The subject was instructed to start the experimentation by using the instrumented hand to press down on a switch located at lap height along the midline of the body. Targets from the predetermined reaching space were presented pseudorandomly to the subject. The subject was told to move to each target at a comfortable, self-determined pace and to grasp the handle for approximately 1 s. After reaching and grasping the target, the subject was instructed to move back to the initial position and press the switch to cue the gantry to move to the next target. The experiment continued until all target locations were reached. Each subject was asked to reach and grasp 400–500 targets, depending on the size of the subject's reaching space. A given target appeared only once in the dataset in order to test the ability of the neural network to generate solutions that would be continuously interpolatable.

The data were low-pass filtered at 4 Hz to remove noise in our motion capture data. The source of this noise was from the environment, likely due to the aluminum gantry required for the experimentation.

Data recorded during the resting periods between target reaches were removed in order to limit the contribution of the initial posture to the training of the neural networks. Data were partitioned into three datasets. First, 20% of the data were set aside as novel validation data. Validation was used after neural network training to quantify the ability of neural networks to generalize for novel data. From the remaining data, 80% of the data points were randomly sampled and set aside as the training dataset. The training set was used during offline training of the neural networks. The remaining data were set aside as a testing set. The testing set was used as novel data with which to test the neural network during training.

C. Design of the Inferential Command System

To position the hand in space, one must be able to flex/extend the elbow appropriately to reach locations in extrapersonal space. In our previous work [11], we found that the three rotational angles S_{FE}, S_{IER}, and S_{ABAD} and shoulder depression elevation SC_{DE} were sufficient to predict the elbow flexion/extension E_{FE} using an ANN (ANN1) during offline analysis. ANN1 was trained on reaches to locations that were 60–100% of the arm length from the body because the correlations between shoulder and elbow posture were weak and inconsistent for targets close to the body. Unsurprisingly, in preliminary VR experiments, it was difficult for subjects to bring objects near the body using only ANN1. Therefore, a second algorithm was developed using elevation of the shoulder for direct, proportional control of flexion of the elbow, based on an observed tendency of subjects to make such movements when the hand was close to the mouth.

Having two control paradigms controlling one joint could prove to be confusing and difficult to use independently by subjects. Likewise, having two separate states, one using a neural network and another using the elevation of the shoulder to control the same output, could yield sudden changes in output when switching between the two control schemes. In order to obtain smooth transitions between them, the two control schemes determining elbow angle were averaged according to reciprocally varying weights (see Fig. 1) based on the distance of the hand from the center of the body. As the hand was brought closer to the body, the subject's shoulder elevation had a stronger influence in determining the flexion of the elbow. Moving distally from the body, the prediction from the ANN dominated the command signal.

Assuming no contribution from the proximal joints, hand orientation is determined by the forearm pronation/supination (FPS) angle, wrist flexion/extension, and wrist deviation. For targets located in front of the body, FPS is used to align the hand with targets rotated in the frontal plane. Wrist flexion/extension and radioulnar deviation RU_{DEV} are used to align the hand in transverse or sagittal planes, depending on the rotation of the hand. Because the targets used in this study were only rotated in the frontal plane, we assumed that only FPS and RU_{DEV} needed to be specified. RU_{DEV} was coupled to the hand posture such that the axis for cylindrical grip (which passes through the knuckles) was made to be parallel with the frontal plane. Thus, FPS was the user-determined output of the ICS responsible for orienting the hand with the targets. FPS was predicted using another ANN (ANN2) from the same shoulder input DOFs as ANN1. Wrist flexion/extension remained fixed at neutral.

The remaining required output is opening/closing of the hand. As discussed in the preceding work, there was no apparent relationship between shoulder posture and the onset of grasp [10].

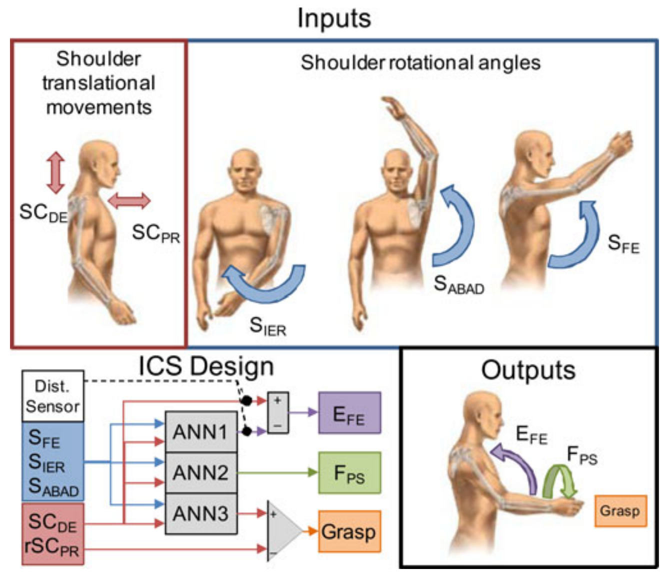

Fig. 1. Schematic of an ICS. The recorded and controlled DOF. Shoulder rotational angles (in blue) are shoulder abduction/adduction S_{ABAD}, shoulder flexion/extension S_{FE}, and shoulder internal/external rotation S_{IER}. Shoulder translational movements (in red) are scapuloclavicular depression/elevation SC_{DE} and scapuloclavicular protraction/retraction SC_{PR}. Outputs of the ICS are elbow flexion/extension (in pink—E_{FE}), FPS (in green—F_{PS}), grasp (in orange), and radioulnar deviation (in purple—RU_{DEV}). Solid lines indicate values dependent on inferences from shoulder posture. Dashed lines show values independently determined from the shoulder posture inferences. Shoulder rotational angles and depression/elevation are used as inputs to the neural networks (ANN1, ANN2, and ANN3). E_{FE} output is determined by a combination of outputs from ANN1 and the SC_{DE} scheme described in the text. The contribution from either ANN1 or SC_{DE} is determined by an estimator measuring the distance from the hand to the body. The closer the hand is to the body, the higher the gain on the output from SC_{DE} scheme and the lower the gain on the output from ANN1. F_{PS} is determined by the output from ANN2. Grasp is determined by SC_{PR}. In certain areas of reaching space, subjects naturally protract their shoulders as a part of the reaching movement. Thus, the natural protraction needs to be deconvolved from the grasping signal. ANN3 predicts the naturally occurring SC_{PR} movement and is subtracted from the value of SC_{PR} recorded during real-time deployment.

Instead, ipsilateral sternoclavicular protraction SC_{PR} was designated to control proportionally the closing of the hand. In preliminary work, we found that subjects would naturally protract their shoulders when reaching to certain targets in space. This would result in an unreliable control paradigm for grasp because the hand would unintentionally close when reaching to such locations. Thus, in order to use SC_{PR} as a reliable control for hand closing, this control movement needed to be deconvolved from the natural protraction–retraction movement associated with reaching toward different positions in space. To this end, a third ANN (ANN3) was trained to predict natural protraction/retraction pSC_{PR} from the same shoulder input DOFs used in the previous two ANNs. The recorded protraction/retraction rSC_{PR} was, then, subtracted from the predicted protraction/retraction pSC_{PR} and multiplied by a gain to obtain the proportional command for hand opening/closing.

D. ANN Training

The three ANNs described previously were created in NeuralWorks Predict (NeuralWare). This software employed an

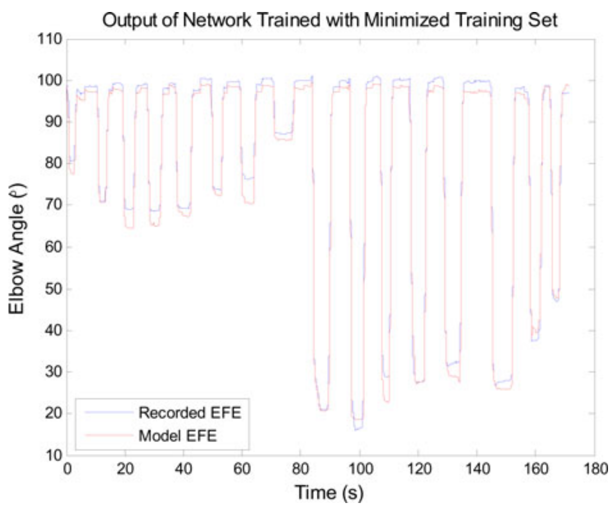

Fig. 2. Output of ANN1. Elbow flexion/extension E_{FE} for a subject is shown in red, whereas the recorded E_{FE} is shown in blue. The predicted output shown is on offline test data. Clearly, there are errors present between the predicted and actual values, but in the study presented here we examine how well can subjects cope with these errors to complete a reach and grasp task.

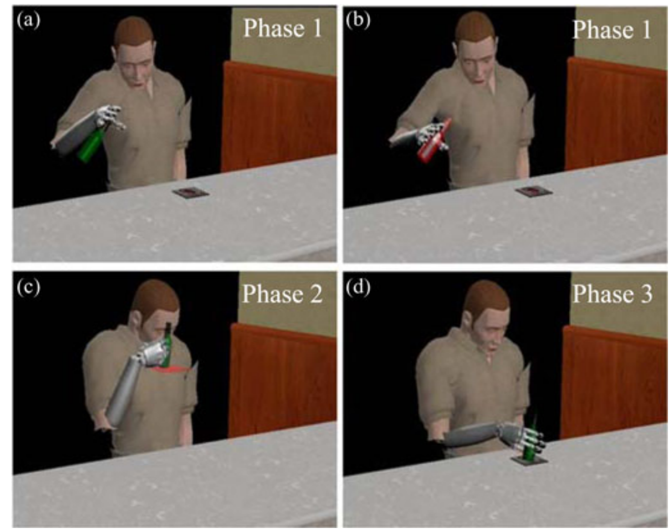

Fig. 3. VR reach and grasp task as seen by an observer. A and B show the first phase of the task. In A, the bottle is in a random position and orientation and the subject is to reach to the bottle. As shown in B, the bottle is highlighted red when the subject has met the appropriate grasp conditions. Once grasped, the coaster on the table is moved to a position near the chin of the virtual human, as seen in C. After the subject holds the bottle near the chin for 3 s, the coaster moves to a position on top of the table. To successfully finish the task, the subject must release the bottle on top of the coaster as shown in D.

adaptive gradient backpropagation algorithm to tune the weights and biases of the ANN to maximize the correlation between the model predictions and the recorded data. To improve the ANNs ability to generalize and to prevent overfitting, the program employed a method of "early stopping," which stopped training of the neural network if the neural network's performance on novel, test data no longer improved. The hidden layer contained units with hyperbolic tangent activation functions. Hidden layer size was automatically determined through a cascade learning algorithm. The coefficient of determination R^2 between the predicted output and recorded output was measured for all the ANNs. Any R^2 value above 0.5 was considered a strong correlation. An example of predicted output of an ANN versus the recorded joint angle is shown in Fig. 2.

Because amputees and tetraplegics are unable to generate reaching movements to train ANNs, it is important to evaluate whether subjects can learn to use a set of neural networks trained with another person's reaching data. To assess this problem, subjects using the ICS alternated between the use of ANNs trained on their own reaching data (within-subject network) and ANNs trained with another subject's data (between-subject networks). To determine which between-subject ANN to use, each subject's set of ANNs was tested on all the validation data from the other subjects. The set of ANNs that predicted a given subject's data the worst during offline analysis was assumed to represent the reaching strategies most foreign to that subject and, therefore, was selected as the between-subject networks for that subject.

E. VR Testing

A simple VR task was developed in the MSMS software environment [15] to evaluate how well subjects could learn to use the ICS. As a simplification, the VRE did not include dynamics or collision detection and instead just represented the kinematics of the movements generated. The task mimicked reaching and grasping a food item, bringing the item near the mouth to consume it, and replacing it on a table (see Fig. 3). The VRE task was broken down into three distinct phases: phase 1—"acquisition," in which the subject reaches and grasps a bottle-shaped object in 3-D virtual space; phase 2—"return," in which the subject brings the bottle to the mouth and holds the bottle in that position for 3 s; and phase 3—"replace," in which the subject releases the bottle on a table at a designated location.

The eight subjects were split evenly into two groups, both of which performed the same set of tasks in the VRE. For the ICS group, the posture of the animated hand was based on the predictions of the ICS according to their shoulder posture; for the Natural Control group, the posture was taken directly from real-time motion capture sensors mounted on the hand and forearm. In order to maintain novelty of the task, we did not crossover subjects between the groups.

Subjects were seated and restrained as in the previous gantry-based reach and grasp task. Sensors were placed on the right arm and calibrated. Additional sensors were placed on the wrist and index fingers of subjects in the Natural Control group to measure the rotational angles of the wrist and opening and closing of the hand, respectively. Subjects donned stereoscopic VR goggles (NVIS, Inc., Reston, VA) equipped with a three-axis accelerometer, a gyroscope, and magnetometer (Microstrain, Inc., Williston, VT) to provide head tracking [16]. The stereoscopic goggles provided subjects with a first-person view within the 3-D VRE. Anthropomorphic virtual human models were scaled to replicate the dimensions of the subject.

In order to grasp the bottle, the subject was required to approach the bottle with an open hand, place the hand within

6 cm of the bottle with velocity of the hand below 1 cm/s, and match the orientation of the hand to the orientation of the bottle to within 30°. Once the grasp conditions were met, the bottle changed color indicating that the bottle could be grasped. Once the bottle was grasped, a square-shaped target (coaster) moved into place near the mouth, showing the subject where to move the bottle next. When the bottle was within 5 cm of the center of the coaster, the coaster was highlighted much like the bottle in the previous phase, indicating that the bottle was in the correct place. After 3 s, the coaster moved to a position on the table in front of the subject. The subject was instructed to reach to the target again, but this time, once in the proper location, the subject was told to release the bottle on top of the coaster. If the subject succeeded in doing so, the bottle was moved to another random position and orientation within the subject's reaching space.

Subjects had 30 s in each phase of the task to complete that phase. If the subject did not complete a given phase in 30 s, the bottle position was reset to the next random starting position and orientation in the queue. Data recorded during a failed trial were discarded, though the occurrence of each failed trial was documented. The experiment was continued until the subject completed the task for 30 trials. Several variables were recorded during each session, including distance between hand and bottle, position of the bottle, time, phase of task, and trial counter. Following each session, subjects were informed of their completion percentage and total time taken to complete the experiment. Subjects were also told about the fastest completion time and highest completion percentage obtained across all subjects, creating an informal competition and motivation to obtain higher completion percentages and faster experiment completion times.

The VRE experiment was conducted for both the ICS group and the Natural Control group subjects over ten sessions. Subjects in the ICS group began using the within-subject networks in session 1 and between-subject networks were used every other session after that. A minimum of 24 h were required between each session.

F. Identifying a Comparative Performance Metric

To compare performances between the ICS group and the Natural Control group subjects in a real-time setting, a unifying metric that expresses performance quantitatively is needed. An obvious metric is the time taken to complete a trial within a session, but time may be dependent on the distance between the hand and bottle at the onset of the session.

To identify if a relationship existed between time and distance, we needed to examine first whether there indeed was a correlation between the two values. A comparison between time and distance is only appropriate in the second (return) phase of the task, because this phase is essentially a point-to-point movement. The scatter plots of time versus distance were highly variable across all sessions for a given subject and across subjects. Data from all eight subjects showed poor correlations between distance and time for phase 2 of the experiment.

It is likely that distance and time are indeed correlated but the correlation is weak due to the variances in endpoint speed. Thus, mean time was chosen as the comparative performance metric. We believe mean time is an appropriate metric because subjects were moving the hand with high velocities and low variations in performance (as shown in the following) by the tenth trial, and so a difference of a few inches in the distance to the target does not yield a significantly different time to reach the target.

TABLE I
COEFFICIENT OF DETERMINATION R^2 FOR BOTH WITHIN- AND BETWEEN-SUBJECT ANNS

Subject	Network Type	E_{FE}	F_{PS}	SC_{PR}
1	Within-subject	0.80	0.55	0.67
	Between-subject	0.45	0.30	0.12
2	Within-subject	0.67	0.75	0.74
	Between-subject	0.01	0.32	0.04
3	Within-subject	0.77	0.65	0.76
	Between-subject	0.25	0.09	0.04
4	Within-subject	0.61	0.75	0.80
	Between-subject	0.06	0.22	0.17

III. RESULTS

Subjects 1–4 were placed in the ICS group and subjects 5–8 were placed in the Natural Control group. The ICS group had mean lower arm lengths of 10.25″ (SD = 0.28″), upper arm lengths of 11.875″ (SD = 0.95″), and clavicle lengths of 6.87″ (SD = 0.25″). The Natural Control group had mean lower arm lengths of 10.50″ (SD = 0.41″), upper arm lengths of 12.38″ (SD = 1.25″), and clavicle lengths of 7.5″ (SD = 0.58″).

A. Offline ANN Performance

Three ANNs were trained for each of the four subjects in the ICS group. Each trained network's offline performance on the respective validation set is shown in Table I. Every within-subject ANN achieved R^2 values greater than 0.5 on the validation set. Also shown in Table I is the performance of the between-subject neural network for each subject. As explained previously, the between-subject network was selected based on how poorly it performed on a given subject's data. Thus, the offline performance was necessarily significantly worse than the within-subject networks.

B. Analysis of Trial Completion Percentage

Because time to perform each phase (see Fig. 3 for definition of phases) was not dependent on distance to target, it was used to compare trials. Time to complete each phase was recorded for each attempt over a period of ten sessions. If the subject was unable to complete a trial, the trial data were discarded. Completion percentage of trials over each of the ten sessions is shown in Fig. 4. The figure contains plots of the ICS group subjects only because all subjects in the Natural Control group maintained a 100% completion percentage over the ten sessions. In the first session, subjects in the ICS group completed the session on average with a completion percentage of 70% (SD = 20%). The same subjects were able to complete on average 98% (SD = 3%) of the trial attempts on the last session, indicating progressive improvement on the task.

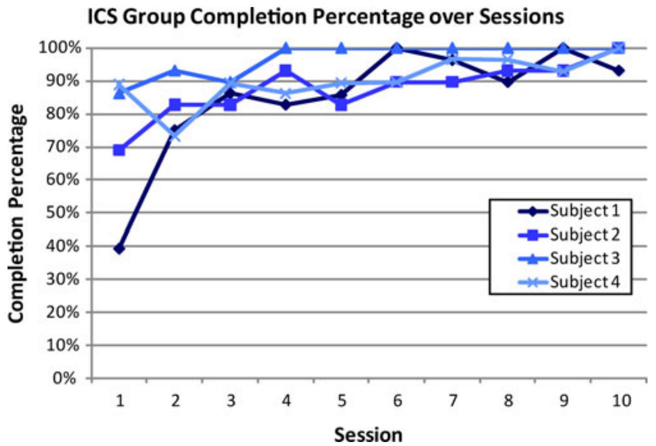

Fig. 4. Plot of completion percentages of trials over sessions for the ICS group subjects. During the first session, none of the subjects in the ICS group completed more than 90% of the trials. In the first session, subject 1 performed the worst with 39% completion rate, while subject 4 performed the best with 89% completion rate. It is also important to note that subjects switched between within- and between- subject networks every other session, but there is no apparent oscillatory trend. All subjects converged to a completion percentage greater than 90% after the fifth session and achieved 100% completion percentage at least once over the ten sessions.

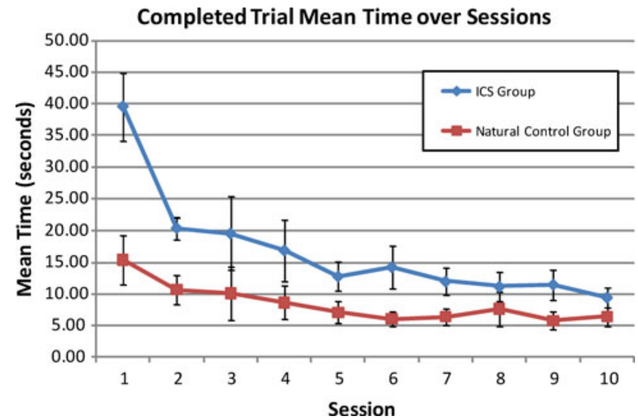

Fig. 5. Plot of trial mean times for both experimental groups over the number of sessions. Mean trial completion times for the ICS group are highlighted in blue, whereas mean times for the Natural Control group are shown in red. In session 1, subjects in the ICS group finished trials with a mean time of 39.52 s (SD = 5.39 s), while subjects in the Natural Control group finished trials with a mean time of 15.40 s (SD = 3.84 s). After the fifth session, the ICS group showed little, very little difference in mean time performance when switching between the within- and between-subject ANNs, suggesting that the use of either network would not significantly affect performance. After ten session, subjects in the ICS group completed trials with a mean time of 9.49 s (SD = 1.52 s), while subjects in the Natural Control group finished with a mean time of 5.76 s (SD = 1.65 s).

To investigate why subjects were missing targets, we searched for similarities across missed targets over the last five sessions (sessions 6–10). Specifically, we looked for trends based on target orientation and target position. In this analysis, we did not include data from subject 3 because this subject maintained a 100% completion percentage over the last five sessions. We found a slight trend suggesting difficulty with the horizontal orientation (90°, which could be reached either by extreme pronation or extreme supination); subjects were not able to grasp this target 15% of the attempts; failure rates were 4% for 45° orientation and 1% for 135° orientation. Subjects were able to grasp the vertical orientation (0°) during every attempt. We also found a trend based on the position of the target. Target locations were placed in bins of equal width with respect to the lateral distance (along the z-axis) from the shoulder center of rotation. Because the extrapersonal space of a given subject was scaled to their limb dimension, the widths of the bins varied from subject to subject. There were a total of six bins: two bins were located to the left of the shoulder center of rotation and four bins were located to the right of the shoulder center of rotation. We found a trend showing that subjects had difficulty with targets located at the edges of the workspace. Specifically, subjects were not able to grasp 17% of targets located in the left-most bin and 11% of targets in the right-most bin. Missed percentage of targets was no greater than 4% (SD = 1%) in the other bins.

C. Comparisons in Trial Mean Times Between Groups

The mean time to complete a trial was compiled from the successfully completed trials for each of the subject's ten sessions. The 3-s holding period during phase 2 was subtracted from the total trial time. The mean time over the ten sessions for all eight subjects is shown in Fig. 5. During the first session, subjects in the ICS group finished trials with a mean time of 39.52 s (SD = 5.39 s), while subjects in the Natural Control group achieved a mean of 15.40 s (SD = 3.84 s). Mean time decreased over time for all subjects in an exponentially decaying fashion. The ICS group subjects showed no apparent tradeoff when switching between the within- and between-subject networks after the sixth session. In the tenth and last session, subjects in the ICS group were able to finish the trials with a mean time of 9.49 s (SD = 1.52 s), while subjects in the Natural Control group finished the trials with a mean time of 5.76 s (SD = 1.65 s).

D. Analysis of Spatial Variability in Performance

While mean times and completion percentage do provide some insights into the quality of the ICS, the analysis is not complete. It was possible that subjects could complete the task very easily for certain positions and orientations but not others. Thus, we examined the mean times across various areas of the workspace over each of the ten sessions. For each session, trial completion times were binned based on the bottle's starting position in space at the onset of a trial. Additionally, the mean time and standard deviation were recorded for each session. In Fig. 6, exemplar mean times are shown as a range of colors for bottle positions in various regions of the *XZ* plane (corresponding to top-down view) over ten sessions. Initially, the subject had difficulty across the entire workspace. Targets located far from the shoulder center of rotation resulted in the largest trial completion times. Over sessions, the subject was able to improve performance across the entire workspace. By the seventh session, the subject maintained mean trial completion times below 20 s across the entire workspace. We also investigated the effect of target orientation on mean time but found no trend across all

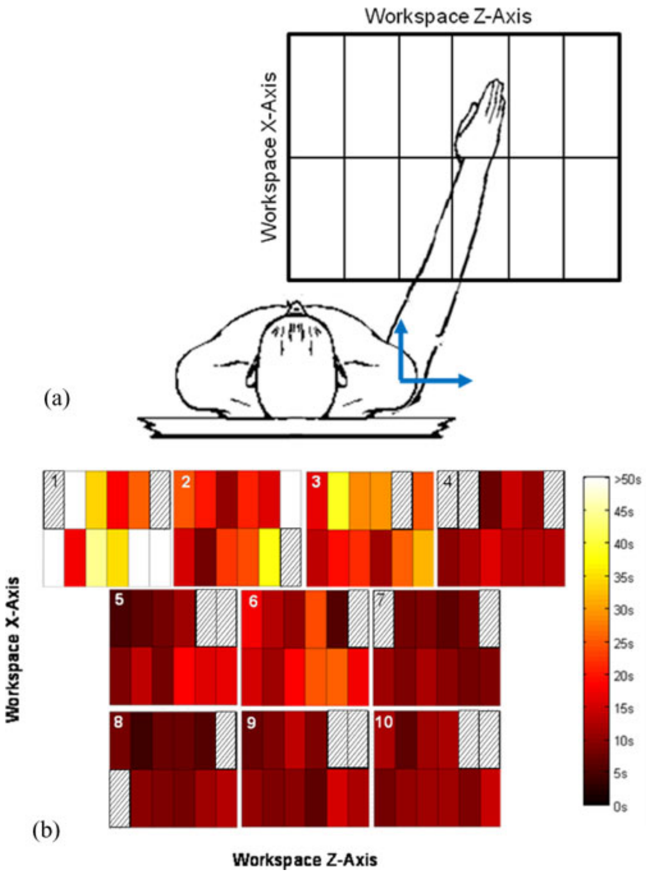

Fig. 6. Analysis of spatial variability in performance over sessions. (A) Workspace was parsed into rectangular blocks. Target position is given with respect to the shoulder center of rotation. The *XZ* plots provide a top-down view of the workspace. (B) Color-scaled plots of subject 3's mean times over blocks of the subject's workspace are shown over ten sessions. Darker colors correspond to faster mean times, while brighter correspond to slower times. If a particular block is crosshatched, it indicates that a target was not presented in that region of workspace to that subject during the session. Session numbers are in bold at the lower left corner of the plots. Initially, the subject performed poorly during session 1 with several areas of mean times over 50 s. With practice, the mean times across the workspace were reduced. By the seventh session, the subject achieved a consistent low mean time across all the blocks of the workspace.

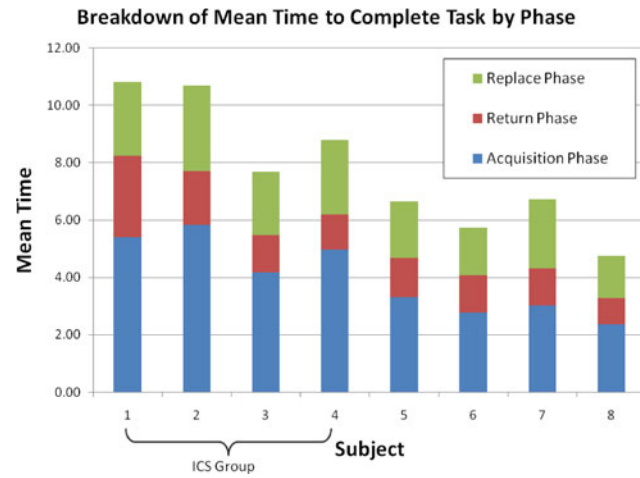

Fig. 7. Breakdown in mean time to complete task by phase for all subjects on the tenth trial. Subjects in the ICS group are indicated by the brackets. Within groups, the variations of time spent in each phase are very minimal. The clear differences between groups are the time spent in the acquisition phase. Times spent in the return and replace phases are very similar across all subjects. This finding was statistically confirmed using a Wilcoxon *t*-test.

ICS group subjects (all mean times for a given orientation were within one standard deviation of other mean times).

E. Identifying Sources of Differences in Performance Between Groups

There was a persistent difference in mean times between the ICS group and the Natural Control group subjects even after training. To get a better understanding of where the difficulties arise for the ICS group subjects, we compared the differences between the two groups in mean time spent in each of the three phases of the VR experiment. Fig. 7 shows a stacked bar graph of the mean time achieved during the tenth trial in the three phases of the task for all eight subjects.

From Fig. 7, it is clear that the largest differences in mean times between the two groups occurred during phase 1 (2.36 s). A Wilcoxon *t*-test analysis confirmed that the groups' performances were significantly different in phase 1 ($P < 0.05$). For phases 2, the mean times were 1.82 (SD $=$ 0.74 s) and 1.10 s (SD $=$ 0.4 s) for the ICS and Natural Control groups, respectively, and not significantly different ($P > 0.05$). For phase 3, the means were 2.59 (SD $=$ 0.32 s) and 2.03 s (SD $=$ 0.90 s) for the ICS and Natural Control groups, respectively, and, likewise, were not significantly different.

F. Sensitivity of the ICS

One advantage of using shoulder posture as opposed to myoelectric command signals is that patients will generally have much higher precision (i.e., more distinguishable states) as a result of kinesthetic feedback from muscle spindles and other proprioceptors. This could provide the basis for the corrective movements that were frequently observed. Thus, it is important to understand how the nonlinear ANNs might transform small changes in their inputs into large changes in their outputs that might limit achievable accuracy.

We conducted a sensitivity analysis on the ANNs at various arm postures and endpoint positions within extrapersonal space. An anthropomorphic model of the human arm was created in Simulink. The arm model included the scapuloclavicular, glenohumeral, elbow, and FPS joints. The arm was scaled to match the dimensions of human subjects in the aforementioned study. ANNs used in the ICS were used to drive the elbow and forearm joints. The input DOFs were specified according to the values recorded during the gantry-based reach and grasp task corresponding to a certain endpoint position. Each of the four input DOFs were varied by $\pm$ 10° at increments of 1° and changes in the endpoint position were measured and plotted (see Fig. 8). The sensitivities of the ANNs were observed as endpoint positions changed in azimuth [see Fig. 8(A) and (B)], elevation [see Fig. 8(C) and 8(D)], and radial distance [see Fig. 8(E) and 8(F)].

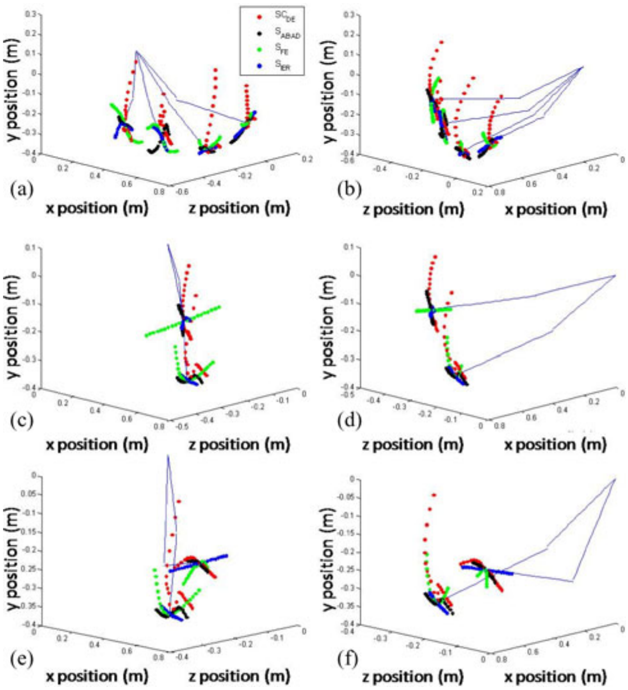

Fig. 8. Sensitivity analyses of the ICS as a function of the input DOF and position in extrapersonal space. The changes in endpoint position with respect to changes in SC_{DE} (shown in red), S_{ABAD} (black), S_{FE} (green), and S_{IER} (blue) inputs are shown. The solid blue lines indicate the upper and lower segments of the arm model. (A) and (B) Two different views (rotated 90° about the *y*-axis) of endpoint positions varying in azimuth. (C) and (D) Two views of arm postures and endpoint positions varying in elevation. (E) and (F) Views of proximal and distal endpoint positions. The distal position in (E) and (F) corresponds to the third position from the left in (A) and (B) and the lower position in (C) and (D). Results indicate that the ICS is most precise at the proximal and medial parts of the workspace but loses precision at the distal and lateral portions of the workspace.

From Fig. 8(A) and (B), it is clear that the ANNs are highly sensitive to most of the input DOFs at the edge of the workspace. As the endpoint moved medially, the sensitivity to changes in the rotational shoulder angles decreased and the changes in endpoint position became linear. Changes in elevation of the endpoint position did not result in a great change in sensitivity of the ANNs. The linearity and orientation of the changes in endpoint positions did vary but the magnitude of the changes did not. As the endpoint position was moved proximally [see Fig. 8(E) and (F)], the sensitivity to shoulder internal/external rotation S_{IER} increased, whereas the sensitivity to shoulder flexion/extension S_{FE} and scapuloclavicular depression/elevation SC_{DE} decreased. Across most of the postures, the ANNs were most sensitive to SC_{DE} and S_{FE}, while changes in S_{IER} and shoulder abduction/adduction S_{ABAD} did not result in large changes in endpoint position.

IV. Discussion

In this study, we examined the use of a noninvasive ICS during a simple, virtual reach-and-grasp task. The kinematics of the task mimicked the consumption of a food item. The objective of this study was twofold: 1) to assess the ability of able-bodied subjects to use the ICS system with ANNs trained with between- and within-subject data; and 2) to compare and quantify the performances of subjects using the ICS versus subjects using complete motion tracking to complete the task.

A. Speed and Accuracy

Examination of the experimental results clearly shows that speed and accuracy performance of the ICS in the VR task is determined by 1) learning to use the VR system in general and 2) learning to compensate for errors and ambiguities of the ICS. The former is highlighted by the fact that in both groups we found that mean time per trial decreased exponentially with practice over the ten experimental sessions. This finding is a typical characteristic of learning [17].

The challenges posed by the ICS can be seen in the difference in performance between the two experimental groups. Overall, the Natural Control group subjects performed 39% faster on average per trial than the ICS group in the final session. Most of the difference in performance time between groups occurred in phase 1 and appeared to be related to difficulty in closing the hand reliably. This was further confirmed by subjective feedback from the subjects. The difficulty could be attributed to the command scheme employed for grasping. When subjects would protract their shoulders forward to close the hand around the bottle, the hand would move forward because of the mechanical linkages between the joints, causing them to miss targets.

In addition, ICS subjects had difficulty with certain targets based on their location in space and the orientation of the target. Specifically, we found that subjects had difficulties reaching to targets that were horizontal and were located at the edges of the reaching space. This is understandable but most likely would not be a problem in a real-world scenario because users could rotate their torsos or wheelchairs to bring the targeted object to a location that is easier to reach.

Finally, we also observed some minor corrective movements once the hand reached the vicinity of the bottle but this was present in both groups of subjects. In the ICS group subjects, these correctives were hard to decouple from the retraction/protraction movements used to open and close the hand. It is likely that most of these correctives are the result of 1) loop delays between the action of the subject and the display of the movement and/or 2) an elective strategy of making quasiballistic movements to be followed by corrective movements as needed based on visual perception. It is important to note that subjects doing these VR tasks attempted to complete the task as fast as possible to get the "fastest time," and there is a well observed tradeoff between speed and accuracy.

B. Generalization Between ANNs

We hypothesized that, irrespective of which set of ANNs (within- or between-subject ANNs) was used, subjects would be able to complete the VR task. Offline analysis showed that the predictive abilities of ANNs did not generalize well to data from other subjects, while within-subject ANNs performed well for all subjects. This might reflect true variability across subjects in their postural synergies. Several studies have shown that the invariant features of reaching such as straight hand trajectories and bell-shaped curves of the tangential hand velocity versus time are preserved across subjects; therefore, it is not likely that the reaching strategies varied greatly between subjects [2], [4]–[7]. Rather, we believe that the ratios between the proximal and distal segments of the arm required subjects to use different patterns of coordination between the joint angles to reach targets presented by the gantry. Additional factors such as a lack of strict control of the subjects' initial posture and overfitting of the ANNs could have also contributed to the poor offline intersubject performance.

Despite the poor offline performance, we assumed that subjects could learn to cope with the errors as long as the errors were not incomprehensible and were predictable. We considered the situation analogous to an experiment by Lacquaniti *et al.*, in which subjects were asked to reach between an initial position and target position after their forearms had been artificially doubled in length by attaching a pole to their forearms [12]. They found that despite the change in the internal constraints of the limb, subjects immediately were able to adjust their shoulder and elbow posture to maintain a straight endpoint path and a bell-shaped endpoint velocity curve. Subjects were able to do this so quickly because they were able to anticipate the errors caused by the length of the forearm and make adjustments in the other joints to minimize those errors. Likewise, we found that subjects could, indeed, learn to cope with errors to control the arm successfully in the VRE. After the sixth session, there was no appreciable difference when subjects switched between within- and between-subject ANNs both in terms of completion percentage and mean trial completion time.

C. Anisotropy of the ICS Across the Workspace

These results from our sensitivity analysis indicate that subjects using the ICS can likely make precise corrections near the proximal and medial parts of the workspace. The precision decreases as the subject moves distally and laterally, but it is likely that subjects will infrequently move to these parts of the workspace. Additionally, small changes in the $\mathrm{SC_{DE}}$ DOF result in large changes in endpoint position but subjects rarely make large $\mathrm{SC_{DE}}$ movements. Furthermore, when using the ICS, subjects are only inclined to make large $\mathrm{SC_{DE}}$ movements when they wish to initiate large movements of the hand to the mouth. While these results indicate that subjects may be able to make precise corrective movements in certain parts of the workspace, it remains to be seen how precisely the ICS can be used for simple real-world tasks such as grasping and transporting a glass of water without spilling its contents.

D. Potential Improvements

1) Grasping Function: There are some potential solutions for improving grasping in the ICS. One method is to include a software solution to compensate for shoulder protraction movement in order to keep the hand in a stable position by adjusting the joints in the arm. This solution is not trivial because the compensation by the joints of the arm varies as a function of the arm posture. Another solution could be to use electromyography (EMG) to proportionally close the hand, similar to the myoelectric technology currently available for upper-limb prostheses. EMG sensors could be placed on the biceps and triceps or another pair of agonist–antagonist muscles, preferably not involved in reaching.

2) Loop Delays: The loop delays in our experimental system were mostly due to the heavy low-pass filtering (third-order Butterworth with 3-Hz cutoff) implemented to reduce 4-Hz noise in the sensors. The noise was related to the Flock of Birds motion capture system and could not be removed at the source. The delay from this filter was approximately 45 ms. The other possible sources of delays are the motion tracking (10 ms), the calculation of predicted outputs from ANNs ($<$ 10 ms), the rendering time for VRE (15 ms), and the refresh rate of the VR goggles (17 ms); but these delays are insignificant compared to the filter delay. It should be possible to design a clinical position sensing system that avoids this noise and the resulting delays. One such technology (described in the following) currently has a lower sampling frequency (10 Hz) but that would actually result in less delay than the filters employed in these experiments.

3) Deploying and Evaluating the ICS With Amputees in Real-World Tasks: In the study presented here, we commented on the quality of the ICS in comparison to the full motion capture of the limb as an analog to a comparison between the performance of amputees and quadriplegics versus able-bodied subjects. In truth, able-bodied subjects using the ICS are not representative of these patients. Able-bodied subjects have proprioceptive information from the entire intact limb available to them as they use the ICS system, whereas amputees and quadriplegics do not currently receive proprioceptive feedback from their prostheses. In addition, several studies have shown that brain areas responsible for movement of the upper limb undergo reorganization in both amputees [20]–[22] and in quadriplegics [23], [24]. A study of reorganization in the motor cortex of transradial amputees who did not wear prostheses revealed that spatial representations of the stump muscles increased in size [25]. The use of a prosthesis with an ICS is likely to induce further changes in cortical representations of the muscles that control the shoulder. Use of the ICS in quadriplegic patients would depend on the details of their sensory and motor loss, which vary considerably among patients. Many patients have a limited range of shoulder motion, particularly in elevation, and possibly limited kinesthesia from sensory loss. We are encouraged by the ability of able-bodied subjects to adjust to ANNs that were trained for other subjects and correlated poorly with the test subject, but loss of ability to reach certain shoulder angles would probably require a procedure to rescale the inputs to the ICS accordingly.

It is important to emphasize that the task presented here did not include dynamics of the prosthetic limb, dynamics of the environment, or collision detection. In a real-world study, the dynamics of the mechatronic or functional electrical stimulation prosthesis will have profound effects on the ICS. Some of those dynamics will complicate motor planning but others may simplify control. For example, the accelerations and velocities of a mechatronic limb may be the limiting factor, reducing the need for overt corrective movements; the natural compliance and viscosity of electrically stimulated muscles may make it easier to capture objects as biological fingers encounter them at suboptimal velocities and orientations. Thus, any prosthetic control scheme must be tested with real patients using real prosthetic systems to perform real tasks with real objects.

E. Implications for Prosthetic Control

In order to control advanced prosthetic limbs with many powered articulations, several alternative control schemes are being researched. These include targeted muscle reinnervation (TMR) [26], [27] and peripheral nerve interfaces [28], [29] for upper-limb amputees, and brain–machine interfaces for both amputees [30] and quadriplegics [31]. Each of these control schemes seeks to bypass the lost peripheral function by obtaining control signals directly from the sources or the conduits of motor function. All of these techniques rely on open-loop bioelectric signals that are subject to internal noise and external interference, thus requiring relatively long integration times to produce reliable commands. All of these techniques require invasive procedures, which can only be justified ethically and financially if the complete prosthetic system achieves a very high level of function in everyday activities. This remains to be demonstrated.

In contrast, the ICS uses intuitive command signals derived from the natural movements of the arm during reaching and transport movements. It requires no invasive procedures or implanted technology. The complete postures of shoulder and sternoclavicular joints can be extracted from three commercially available, three-axis microelectromechanical system sensors ($9 \times 9 \times 2$ mm; Honeywell HMC6343) affixed to the sternum, acromion, and transhumeral socket. It can be used by itself for simple but important tasks, as a "fall-back" if more advanced interfaces fail, or to complement and compensate for the inherent noisiness and delays associated with bioelectric command signals. The obvious limitations of the ICS system should be considered in this light. Most transhumeral sockets do not obtain sufficient coupling to the humerus to provide the full range of voluntary axial rotation as assumed in the modeled system, so it may be necessary to use an angulation osteotomy [32] to achieve this. Alternatively, a fixed magnet implanted into the humeral stump could drive the magnetometer in the sensor in the socket to detect relative motion as a command signal. The ICS system cannot provide the user with independent control of the elbow, forearm, or wrist joints or individual fingers. The posture of these joints is dependent on the posture of the shoulder. This likely will not be a problem when reaching but independent control of joints may be necessary for certain tasks such as turning a doorknob. The ICS system is also limited to restoring power grasp to the user. Other grasping patterns cannot be selected without some external switching mechanism.

Many of the limitations of the ICS and other control paradigms can be overcome by combining them into integrated prosthetic systems. One solution could be to couple the ICS with TMR for transhumeral amputees. In this solution, much of the cognitive burden associated with the reaching and transport movements using TMR would be relieved with the use of the ICS, while concurrently retaining the ability to select a specific hand posture or to override the ICS output to move an individual joint independently when necessary. The system provided to any given patient must be tailored to his/her actual injuries, physical condition, activities of daily living, tolerance for invasive procedures, and physical appearance and operator interactions associated with different types of technology. Apparently, competing technologies such as ICS and myoelectric control may best be deployed together, with the strengths of one compensating for the weaknesses of the other.

REFERENCES

[1] E. Biddiss and T. Chau, "Upper-limb prosthetics: Critical factors in device abandonment," *Amer. J. Phys. Med. Rehabil./Assoc. Acad. Physiatrists*, vol. 86, pp. 977–987, Dec. 2007.
[2] M. J. Hollerbach and T. Flash, "Dynamic interactions between limb segments during planar arm movement," *Biol. Cybern.*, vol. 44, pp. 67–77, 1982.
[3] P. Morasso, "Three dimensional arm trajectories," *Biol. Cybern.*, vol. 48, pp. 187–194, 1983.
[4] P. Morasso, "Spatial control of arm movements," *Exp. Brain Res.*, vol. 42, pp. 223–227, Apr. 1981.
[5] J. F. Soechting and F. Lacquaniti, "Invariant characteristics of a pointing movement in man," *J. Neurosci.*, vol. 1, pp. 710–720, Jul. 1981.
[6] T. Flash and N. Hogan, "The coordination of arm movements: An experimentally confirmed mathematical model," *J. Neurosci.*, vol. 5, pp. 1688–1703, Jul. 1985.
[7] W. Abend, E. Bizzi, and P. Morasso, "Human arm trajectory formation," *Brain*, vol. 105, pp. 331–348, Jun. 1982.
[8] J. F. Soechting, C. A. Buneo, U. Herrmann, and M. Flanders, "Moving effortlessly in three dimensions: Does Donders' law apply to arm movement?," *J. Neurosci.*, vol. 15, pp. 6271–6280, Sep. 1995.
[9] M. Desmurget, C. Prablanc, Y. Rossetti, M. Arzi, Y. Paulignan, C. Urquizar, and J. C. Mignot, "Postural and synergic control for three-dimensional movements of reaching and grasping," *J. Neurophysiol.*, vol. 74, pp. 905–910, Aug. 1995.
[10] R. R. Kaliki, R. Davoodi, and G. E. Loeb, "Prediction of distal arm posture in 3-D space from shoulder movements for control of upper limb prostheses," *Proc. IEEE*, vol. 96, no. 7, pp. 1217–1225, Jul. 2008.
[11] R. R. Kaliki, R. Davoodi, and G. E. Loeb, "Prediction of elbow trajectory from shoulder angles using neural networks," *Int. J. Comput. Intell. Appl.*, vol. 7, pp. 333–349, 2008.
[12] F. Lacquaniti, J. F. Soechting, and C. A. Terzuolo, "Some factors pertinent to the organization and control of arm movements," *Brain Res.*, vol. 252, pp. 394–397, Dec. 1982.
[13] D. A. Hong, D. M. Corcos, and G. L. Gottlieb, "Task dependent patterns of muscle activation at the shoulder and elbow for unconstrained arm movements," *J. Neurophysiol.*, vol. 71, pp. 1261–1265, Mar. 1994.
[14] R. Shadmehr and F. A. Mussa-Ivaldi, "Adaptive representation of dynamics during learning of a motor task," *J. Neurosci.*, vol. 14, pp. 3208–3224, May 1994.
[15] R. Davoodi, C. Urata, M. Hauschild, M. Khachani, and G. E. Loeb, "Model-based development of neural prostheses for movement," *IEEE Trans. Biomed. Eng.*, vol. 54, no. 11, pp. 1909–1918, Nov. 2007.
[16] M. Hauschild, R. Davoodi, and G. E. Loeb, "A virtual reality environment for designing and fitting neural prosthetic limbs," *IEEE Trans. Neural Syst. Rehabil. Eng.*, vol. 15, no. 1, pp. 9–15, Mar. 2007.
[17] C. Hovland, "Human learning and retention," in *Handbook of Experimental Pyschology,* S. S. Stevens, Ed. New York: Wiley, 1951, pp. 613–689.
[18] J. R. Lackner and P. Dizio, "Rapid adaptation to Coriolis force perturbations of arm trajectory," *J. Neurophysiol.*, vol. 72, pp. 299–313, Jul. 1994.
[19] N. Wettels, V. J. Santos, R. S. Johansson, and G. E. Loeb, "Biomimetic tactile sensor array," *Adv. Robot.*, vol. 22, pp. 829–849, Aug. 2008.
[20] L. G. Cohen, S. Bandinelli, T. W. Findley, and M. Hallett, "Motor reorganization after upper limb amputation in man: A study with focal magnetic stimulation," *Brain*, vol. 114, pp. 615–627, Feb. 1991.
[21] S. Roricht, B. Meyer, L. Niehaus, and S. A. Brandt, "Long-term reorganization of motor cortex outputs after arm amputation," *Neurology*, vol. 53, pp. 106–111, Jul. 1999.
[22] H. Flor, T. Elbert, W. Mühlnickel, C. Pantev, C. Wienbruch, and E. Taub, "Cortical reorganization and phantom phenomena in congenital and traumatic upper-extremity amputees," *Exp. Brain Res.*, vol. 119, pp. 205–212, Feb. 1998.

[23] O. Raineteau and M. E. Schwab, "Plasticity of motor systems after incomplete spinal cord injury," *Nature Rev. Neurosci.*, vol. 2, pp. 263–273, Apr. 2001.

[24] M. Bruehlmeier, V. Dietz, K. L. Leenders, U. Roelcke, J. Missimer, and A. Curt, "How does the human brain deal with a spinal cord injury?," *Eur. J. Neurosci.*, vol. 10, pp. 3918–3922, Dec. 1998.

[25] K. Irlbacher, B. Meyer, M. Voss, S. A. Brandt, and S. Röricht, "Spatial reorganization of cortical motor output maps of stump muscles in human upper-limb amputees," *Neurosci. Lett.*, vol. 321, pp. 129–132, Mar. 2001.

[26] T. A. Kuiken, G. A. Dumanian, R. D. Lipschutz, L. A. Miller, and K. A. Stubblefield, "The use of targeted muscle reinnervation for improved myoelectric prosthesis control in a bilateral shoulder disarticulation amputee," *Prosthet. Orthot. Int.*, vol. 28, pp. 245–253, Dec. 2004.

[27] T. A. Kuiken, G. Li, B. A. Lock, R. D. Lipschutz, L. A. Miller, K. A. Stubblefield, and K. B. Englehart, "Targeted muscle reinnervation for real-time myoelectric control of multifunction artificial arms," *J. Amer. Med. Assoc.*, vol. 301, pp. 619–628, Feb. 2009.

[28] G. S. Dhillon and K. W. Horch, "Direct neural sensory feedback and control of a prosthetic arm," *IEEE Trans. Neural Syst. Rehabil. Eng.*, vol. 13, no. 4, pp. 468–472, Dec. 2005.

[29] G. S. Dhillon, S. M. Lawrence, D. T. Hutchinson, and K. W. Horch, "Residual function in peripheral nerve stumps of amputees: Implications for neural control of artificial limbs," *J. Hand Surg.*, vol. 29, pp. 605–615, Jul. 2004.

[30] J. K. Chapin, K. A. Moxon, R. S. Markowitz, and M. A. Nicolelis, "Real-time control of a robot arm using simultaneously recorded neurons in the motor cortex," *Nature Neurosci.*, vol. 2, pp. 664–670, Jul. 1999.

[31] C. T. Moritz, S. I. Perlmutter, and E. E. Fetz, "Direct control of paralysed muscles by cortical neurons," *Nature*, vol. 456, pp. 639–642, Dec. 2008.

[32] E. Marquardt, E. and G. Neff, "The angulation osteotomy of above-elbow stumps," *Clin. Orthop. Related Res.*, vol. 104, pp. 232–238, 1974.

Rahul R. Kaliki received the B.S. degree in biomedical engineering from the University of California, San Diego, in 2004, and the M.S. and Ph.D. degrees from the University of Southern California, Los Angeles, in 2009, where the thesis research involved studying the use of shoulder kinematics as a means to predict and control distal joint angles of the upper limb to restore functionality to transhumeral amputees and C5/C6 spinal cord injury patients.

He is currently the Chief Executive Officer of Infinite Biomedical Technologies, Baltimore, MD, where his research is focused on the development and commercialization of control mechanisms and algorithms for transradial prostheses. He is also a Visiting Scientist in the Department of Biomedical Engineering, The Johns Hopkins University, Baltimore. His research interests include neural prosthetics, reanimation of paralyzed limbs, upper-limb prostheses, and motor control.

Rahman Davoodi received the B.Sc. degree in mechanical engineering and the M.Sc. degree in biomechanical engineering from the Sharif University of Technology, Tehran, Iran, and the Ph.D. degree in biomedical engineering from the University of Alberta, Edmonton, AB, Canada.

He is currently a Research Assistant Professor in the Department of Biomedical Engineering, University of Southern California, Los Angeles. His current research is focused on the use of movement neural prostheses to restore normal daily living activities such as standing, walking, reaching, and grasping to the paralyzed and amputee patients. To enable smooth and coordinated man–machine interactions in these movement neural prostheses, he has developed innovative machine-learning control systems. As a systematic alternative to traditional ad hoc design methods, he has developed a number of modeling software and virtual reality environments to model, simulate, and virtually prototype neural prostheses at various stages of development including the optimization of the mechanical design of the prosthesis, the simulation of its physically realistic movements in response to patients commands, and the clinical fitting of the prosthesis by training and rehabilitation of patients in virtual reality environments. He has combined the modeling software with virtual reality hardware to develop physically realistic games and applications to train the patients to effectively operate their movement neural prostheses and enable the victims of stroke and other central nervous system injuries to practice and acquire new motor skills in a safe and motivating environment.

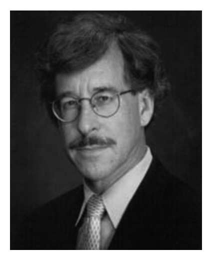

Gerald E. Loeb (M'04–SM'07) received the B.A. and M.D. degrees from the Johns Hopkins University, Baltimore, MD, in 1969 and 1972, respectively, and did one year of surgical residency at the University of Arizona, Tucson.

During 1973–1988, he was in the Laboratory of Neural Control, National Institutes of Health. During 1988–1999, he was a Professor of physiology and biomedical engineering at Queen's University, Kingston, ON, Canada. He is currently a Professor of biomedical engineering and the Director of the Medical Device Development Facility, University of Southern California, Los Angeles. He was one of the original developers of the cochlear implant to restore hearing to the deaf and was a Chief Scientist for Advanced Bionics Corporation from 1994 to 1999, manufacturers of the Clarion cochlear implant. He is the holder of 49 issued U.S. patents and author of more than 200 scientific papers. Most of his current research is focused toward sensorimotor control of paralyzed and prosthetic limbs. His research team has developed BION injectable neuromuscular stimulators and has been conducting several pilot clinical trials. His team is involved in the development and commercialization of biomimetic tactile sensor for robotic and prosthetic hands (www.SynTouchLLC.com). His team is also involved in the development of computer models of musculoskeletal mechanics and the interneuronal circuitry of the spinal cord, which facilitates control and learning of voluntary motor behaviors by the brain. These projects build on his long-standing basic research into the properties and natural activities of muscles, motoneurons, proprioceptors, and spinal reflexes.

Dr. Loeb is a Fellow of the American Institute of Medical and Biological Engineers.